Journal of
Composites Science

MDPI

Article

Effects of Poly(Vinylidene Fluoride-co-Hexafluoropropylene) Nanocomposite Membrane on Reduction in Microbial Load and Heavy Metals in Surface Water Samples

Lutendo Evelyn Macevele [1], Kgabo Lydia Maureen Moganedi [2] and Takalani Magadzu [1,*]

[1] Department of Chemistry, University of Limpopo, Mankweng, Private Bag X1106, Sovenga 0727, South Africa; lutendo.macevele@ul.ac.za
[2] Department of Biochemistry, Microbiology and Biotechnology, University of Limpopo, Mankweng, Private Bag X1106, Sovenga 0727, South Africa; kgabo.moganedi@ul.ac.za
* Correspondence: takalani.magadzu@ul.ac.za; Tel.: +27-015-268-3058

Abstract: In this work, nanocomposite membranes were prepared using silver nanoparticles (Ag) attached to poly(amidoamine) dendrimer (P)-functionalised multi-walled carbon nanotubes (CNTs) blended with poly(vinylidene fluoride-co-hexafluoropropene) (PVDF-HFP) polymeric membranes (i.e., AgP-CNT/PVDF-HFP) via the phase inversion method. The nanocomposites were characterised and analysed via transmission electron microscopy (TEM), scanning electron microscopy (SEM), energy-dispersive spectroscopy (EDX), thermal gravimetric analysis (TGA) and Brunauer–Emmett–Teller (BET) analysis. The TEM and EDX analyses confirmed the presence of Ag nanoparticles on the nanocomposites, while the SEM and BET data showed the spongy morphology of the nanocomposite membranes with improved surface areas. The sample analysis of surface water collected from the Sekhukhune district, Limpopo Province, South Africa indicated that the water could not be used for human consumption without being treated. The nanocomposite membranes significantly reduced the physicochemical parameters of the sampled water, such as turbidity, TSS, TDS and carbonate hardness, to 4 NTU, 7 mg/L, 7.69 mg/L and 5.9 mg/L, respectively. Significant improvements in microbial load (0 CFU/mL) and BOD (3.0 mg/L) reduction were noted after membrane treatment. Furthermore, toxic heavy metals such as chromium, cadmium and nickel were remarkably reduced to 0.0138, 0.0012 and 0.015 mg/L, respectively. The results clearly suggest that the AgP-CNT/PVDF-HFP nanocomposite membrane can be used for surface water treatment.

Keywords: poly(amidoamine); nanocomposite membrane; surface water; filtration; physicochemical; microbial; heavy metals

Citation: Macevele, L.E.; Moganedi, K.L.M.; Magadzu, T. Effects of Poly(Vinylidene Fluoride-co-Hexafluoropropylene) Nanocomposite Membrane on Reduction in Microbial Load and Heavy Metals in Surface Water Samples. *J. Compos. Sci.* **2024**, *8*, 119. https://doi.org/10.3390/jcs8040119

Academic Editor: Francesco Tornabene

Received: 16 November 2023
Revised: 12 January 2024
Accepted: 29 February 2024
Published: 23 March 2024

1. Introduction

Inadequate access to clean water remains a major challenge in many developing countries, affecting mostly rural areas. The majority of people living in developing and underdeveloped countries rely greatly on surface water as their primary source of water for domestic usage due to a lack of potable water supplies. The consumption of polluted water may cause waterborne diseases such as typhoid, diarrhoea, dysentery, cholera and organ damage, which lead to acute health challenges throughout society, heavily impacting children below five years of age [1,2]. These diseases are caused by the ingestion of water contaminated with microscopic organisms (such as viruses and bacteria), disinfection by-products and heavy metals [3,4]. These contaminants have rapidly increased within the surface water due to modern agricultural, household and industrial activities. Microbials such as coliforms, *Escherichia coli* (*E. coli*) and Enterobacteriaceae are used as water quality indicators when assessing the safety of water for human consumption [5]. The determination of the quality of potable water should be performed by assessing its physical, chemical and biological characteristics before usage. These are analysed against the standards for

drinking water outlined by the World Health Organization (WHO) and the South African National Standard (SANS 241) [6–8].

Amongst the heavy metals associated with severe health effects [9] are nickel (Ni), cadmium (Cd), chromium (Cr), iron (Fe), zinc (Zn) and copper (Cu). Although the Fe, Cu and Zn heavy metals play an essential role in the human body, at high concentrations, these metals can lead to severe health complications (such as diabetes, vomiting, liver damage and kidney disease), which are mainly associated with exposure to toxic metals like Cr(VI), Ni and Cd [10,11]. Recent reports from various studies have noted higher-than-normal concentrations of Cr, Fe, Ni and Zn in water collected from the Olifants [12] and Dzindi [13] rivers, as well as from wastewater treatment in Durban, South Africa [9].

Ahmed et al. [14] synthesised silver nanoparticles, and their results revealed a decrease in the concentrations of various physicochemical parameters (converted into per-centages) of textile effluents, such as pH (65%), electrical conductivity (55%), hardness (58%), total suspended solids (TSS) (75%), biological oxygen demand (BOD) (66%) and total dissolved solids (TDS) (76%). Mustapha et al. [15] showed that kaolin/ZnO nanocomposites had improved adsorption performance, with the largest reductions in the chemical oxygen demand (COD) (95%), BOD (94%), Fe(III) (98%), Cr(VI) (100%) and chloride (78%) [15]. In another study by Fanta et al. [16], a synthesised copper-doped zeolite composite adsorbent effectively reduced Cd to 0.005 mg/L (99%), Cr to undetectable levels and BOD to 6.54 mg/L (70%) in wastewater collected from the Akaki river. Although some of the above studies achieved undetectable levels of chromium, the reported cadmium concentration levels are still above the acceptable limits indicated by the WHO [6] and SANS 241 [8] guidelines. It is, therefore, necessary to ensure that the developed composite material is able to reduce both the physicochemical parameters and heavy metal levels to below the acceptable limits.

Although various water purification methods exist today, they are usually too expensive to be implemented by ordinary citizens due to their excessive usages rates and/or a lack of technical operational skills [2]. Common processes such as sand filtration, settlement, coagulation and chlorination are usually utilised for the treatment of contaminated water in various industries, although it is still a challenge for purified water to meet the drinking water standards [17]. This highlights the importance of extensive research to develop improved and low-cost water purification methods that utilise less energy [17]. A solution to the scarcity of safe drinking water would be to find economic methods of purifying surface water for domestic usage.

Somma et al. [18] reviewed a variety of water purification methods, such as adsorption, membrane separation, bioremediation, etc., and noted that adsorption seemed to be the preferred method due to its simplicity and cost-effectiveness. Although the adsorption technique is useful, especially with regard to fast preparation processes, membrane technology also offers some advantages. For example, membrane technology is a useful technique for the removal of organic and inorganic water contaminants. It works by providing a selective barrier that allows certain substances, called the permeate, to pass through, while leaving behind other substances (retentate). Zhang et al. [19] utilised graphene oxide quantum dots to produce thin film nanocomposite (TFN) membranes for the treatment of water polluted by the methylene blue and Congo red dyes. The results showed good antifouling properties and approximately 99% removal efficiency for both the methylene blue and Congo red dyes. Wei et al. [20] purified water polluted by several phthalates using hollowfibre nanofiltration membranes. Good removal efficiency of up to 95% for both di-n-octylphthalate and diethylhexyl phthalate was obtained.

In our previous studies [21], the Ag-MWCNT/PVDF-HFP nanocomposite membrane exhibited good fouling resistance, microbial load reduction (100%), non-leaching properties and excellent bactericidal effects in simulated water samples. The addition of poly(amidoamine) dendrimers, with their highly branched 3D structures, is an excellent choice for the functionalisation of carbon materials, as well as metal ion complexing; these improve the overall surface areas of nanocomposite materials [22,23]. Studies have indi-

cated that carbon materials functionalised with poly(amidoamine) dendrimer encapsulated with silver nanoparticles show better solubility and antibacterial properties [24–26].

Herein, we prepared a nanocomposite membrane containing Ag nanoparticles attached to P-CNT/PVDF-HFP. The study aimed at evaluating the microbial reduction, some physicochemical parameters and the heavy metals within surface water samples collected from the Sekhukhune Municipality, Limpopo Province, South Africa. The effects of the first-generation poly(amidoamine) dendrimer on the dispersity of Ag nanoparticles and performance of the entire nanocomposite membrane were investigated during the surface water analysis.

2. Materials and Methods

2.1. Materials

All chemicals were utilised as received, unless otherwise stated, and were of analytical reagent grade. Poly(vinylidene fluoride-co-hexafluoropropene), polyethylene glycol, silver nitrate, nitric acid, multi-walled carbon nanotubes (CNTs), N,N-dimethylacetamide (DMAC), polyvinylpyrrolidone (PVP), sulphuric acid, ethylenediamine, toluene 2,4-diisocyanate, methanol, methyl acrylate and ethanol were all purchased from Merck, Modderfontein, South Africa.

2.2. Methods

2.2.1. Preparation of AgCNT/PVDF-HFP Nanocomposite Membranes

Functionalised CNTs and dendritic multi-walled carbon nanotubes were prepared using a method reported in the literature [25]. A PVDF-HFP membrane blended with Ag-doped MWCNTs (i.e., 2.5 wt.% AgCNT) was prepared via the phase inversion technique, as described in the literature, to form the AgCNT/PVDF-HFP nanocomposite membrane [27].

2.2.2. Preparation of AgPCNT/PVDF-HFP Nanocomposite Membranes

For the preparation of PVDF-HFP blended with Ag and the poly(amidoamine) MWCNT nanocomposite (i.e., 1.8 wt.% AgPCNT), the procedure was as follows: PVDF-HFP (2 g) was dissolved in N,N-dimethylacetamide (15 mL) at 85 °C while stirring and this was followed by the addition of PVP (0.6 g). The mixture was stirred for 2 h at 85 °C to obtain a PVDF-HFP polymer solution.

In a separate container, silver poly(amidoamine) multi-walled carbon nanotubes (AgPCNTs) (0.037 g) were sonicated in 5 mL of N,N-dimethylacetamide for a period of 30 min. The sonicated AgPCNTs were then added to the PVDF-HFP polymer solution and this was stirred for an additional 1 h. The resultant polymer was then hand-cast in a glass plate using a casting knife at 180 µm thickness. The membrane formed (AgP-CNT/PVDF-HFP) was pre-dried in an oven at 55 °C for about 35 s to pre-evaporate the water, and this was followed by coagulation in a water bath (6 °C) and drying on paper sheets.

2.3. Characterisation of Nanocomposite Membranes

The TEM analysis of the nanocomposites was performed on a JEOL JEM-2100 transmission electron microscope operated at 200 kV. The morphologies of the membranes were examined using a focused ion beam scanning electron microscope (Auriga Zeiss-39-42 SEM with Germini FE-SEM column). The EDS analysis of the nanocomposite membranes was undertaken using a focused ion beam scanning electron microscope. The BET analysis was undertaken on a Micromeritics ASAP 2020 instrument, to investigate the surface properties of the nanocomposite membranes. The thermal gravimetric analysis was performed using the TGA Q500 (V20.13 Build 39) by heating the samples from 30 to 800 °C at a ramping rate of 10 °C/min under nitrogen gas.

2.4. Permeation Tests of Nanocomposite Membranes

To study the swellability of the PVDF-HFP nanocomposite membranes, the membranes were initially weighed on a weighing balance, followed by soaking in distilled water for 7 h before weighing again.

The swellability (Q_t) was calculated as follows:

$$Q_t(\%) = \frac{\left(\frac{m_w}{M_r}\right)}{m_c} \times 100 \quad (1)$$

where m_c and m_w are the initial and final masses of the membrane in g before and after soaking in distilled water. The water content and porosity measurements were performed by immersing the nanocomposite membranes in distilled water, followed by weighing the wet membrane (W_0) after 24 h. The wet membrane was dried in an oven for 24 h at 85 °C, followed by weighing again to determine the dry weight (W_1).

The water content (WC) was calculated using the equation below:

$$WC(\%) = \frac{(W_0 - W_1)}{W_0} \times 100 \quad (2)$$

Porosity (P) was calculated as follows:

$$P(\%) = \frac{(W_0 - W_1)}{Ahd} \times 100 \quad (3)$$

where A is the surface area of the nanocomposite membrane, h is the thickness of the membrane and d is the water density at room temperature.

2.5. Surface Water Analysis

2.5.1. Water Sampling

The collection of surface water (into sterile bottles) for analysis in this study was conducted at 3 different locations, which were the Makotswane dam, Olifants river (near the Flag Boshielo dam) and a furrow in Apel Cross in the Sekhukhune district, Limpopo Province, South Africa. These water sources were used by the local and nearby communities for domestic purposes. The water samples were collected into previously sterilised bottles and placed on ice before analysis in the Microbiology Laboratory at the University of Limpopo. The pooled water samples collected from these areas were analysed within 4 h of sampling, and the pooled water samples for selected heavy metal analysis were preserved in 1% nitric acid.

2.5.2. Physicochemical Properties

Physicochemical parameters such as turbidity, water hardness and colour were analysed using the UV Nanocolor® spectrophotometer (Macherey-Nagel, Düren, Düren). The total suspended solids (TSS) (mg/L) was measured using a gravimetric method reported elsewhere [28].

The TSS solids was calculated as follows:

$$TSS = \frac{(A - B)}{C} \times 1000 \quad (4)$$

where A and B are the initial and final weights of the membrane (in g) before and after filtration, respectively, and C indicates the filtered water volume (in mL). A multi-parameter analyser (HI 991300 pH/EC/TDS meter) was used for the pH, total dissolved solids (TDS) and conductivity measurements.

The calculation of the TDS was as follows:

$$TDS = \frac{(A - B)}{C} \times 1000 \quad (5)$$

where A and B are the initial and final weights of the beaker before and after evaporation (g), while the evaporated water sample (in mL) is indicated by C.

The fold decrease (FD) was calculated as follows:

$$FD = \frac{A}{B} \tag{6}$$

where A and B are the initial and final parameters (i.e., concentration), respectively.

2.5.3. Microbiological and Elemental Analysis of Treated Water Using Synthesised Membranes

The prepared nanocomposite membranes were used to filter 100 mL water samples. The microbiological analysis included the measurement of *E. coli*, total coliforms, Enterobacteriaceae and the aerobic count, performed before and after filtration. The BOD_5 experiment was conducted following the manufacturer's instructions (UV/Vis Nanocolor user manual). The BOD_5 measurements of the control mixture were performed immediately and that of the sample was performed after 5 days, also using the UV/Vis NANOCOLOR® spectrometer. The elemental analysis of the water samples before and after treatment was performed using atomic adsorption spectroscopy (AAS). The metal percentage reduction was calculated as follows:

$$\%reduction = \frac{\left(C_i - C_f\right)}{C_i} \times 100 \tag{7}$$

where C_i and C_f are the initial and final concentrations, respectively.

3. Results

3.1. Characterisation of Nanocomposites and Nanocomposite Membranes

3.1.1. TEM Analysis of AgCNT and AgP-CNT Nanocomposites

Figure 1 shows the TEM images of the AgCNT and AgP-CNT nanocomposites. Both the AgCNT (Figure 1a1) and AgP-CNT (Figure 1b1) composites showed spherical dark spots of Ag nanoparticles attached to MWCNTs and P-CNTs [29,30]. The Ag nanoparticles and the multi-walled CNTs' structures were clearly visible at the high TEM magnifications of the composites (Figure 1a2,b2). The Ag nanoparticles were homogeneously distributed on the P-CNT nanocomposite (Figure 1b1), as compared to the AgCNTs (Figure 1a1). The TEM images showed that the poly(amidoamine) dendrimer on the surface of the MWCNTs contributed to the high dispersity of the Ag nanoparticles, due to their attachments at the ends of the amine groups of poly(amidoamine). The dendrimer further contributed to the smaller Ag nanoparticles of 5.4 nm (as measured from Figure 1b2), as compared to 6.7 nm recorded for the AgCNTs.

3.1.2. SEM Analysis of AgCNT/PVDF-HFP and AgP-CNT/PVDF-HFP Nanocomposite Membranes

The SEM images in Figure 2 show the morphologies of the PVDF-HFP, AgCNT/PVDF-HFP and AgP-CNT/PVDF-HFP nanocomposite membranes. The SEM image of AgCNT/PVDF-HFP (Figure 2b1) shows some surface roughness with the addition of AgCNTs on PVDF-HFP; the roughness increased even further on AgP-CNT/PVDF-HFP (Figure 2c1) with the addition of the poly(amidoamine) dendrimer. Both composites had a rough surface when compared to that of the PVDF-HFP membrane (Figure 2a1), as noted in the literature [31]. A small percentage of MWCNTs and Ag nanoparticles was embedded within the structure of the PVDF-HFP membrane; hence, they were not visible on the surface. The SEM cross-section of PVDF-HFP (Figure 2a2) showed finger-like pores linked to the spongy walls of the membrane. As observed from the cross-sections in Figure 2b2,c2, the presence of AgCNTs and AgP-CNTs on PVDF-HFP slightly increased the surface roughness of the membranes. This resulted in the slight suppression of macrovoids, which

is beneficial for water purification, as reported in the literature [32,33]. The EDX analysis of AgCNT/PVDF-HFP (Figure 2d1) and AgP-CNT/PVDF-HFP (Figure 2d2) confirmed the presence of both Ag nanoparticles and functional groups, such as oxygen, attached to the surfaces of the MWCNTs.

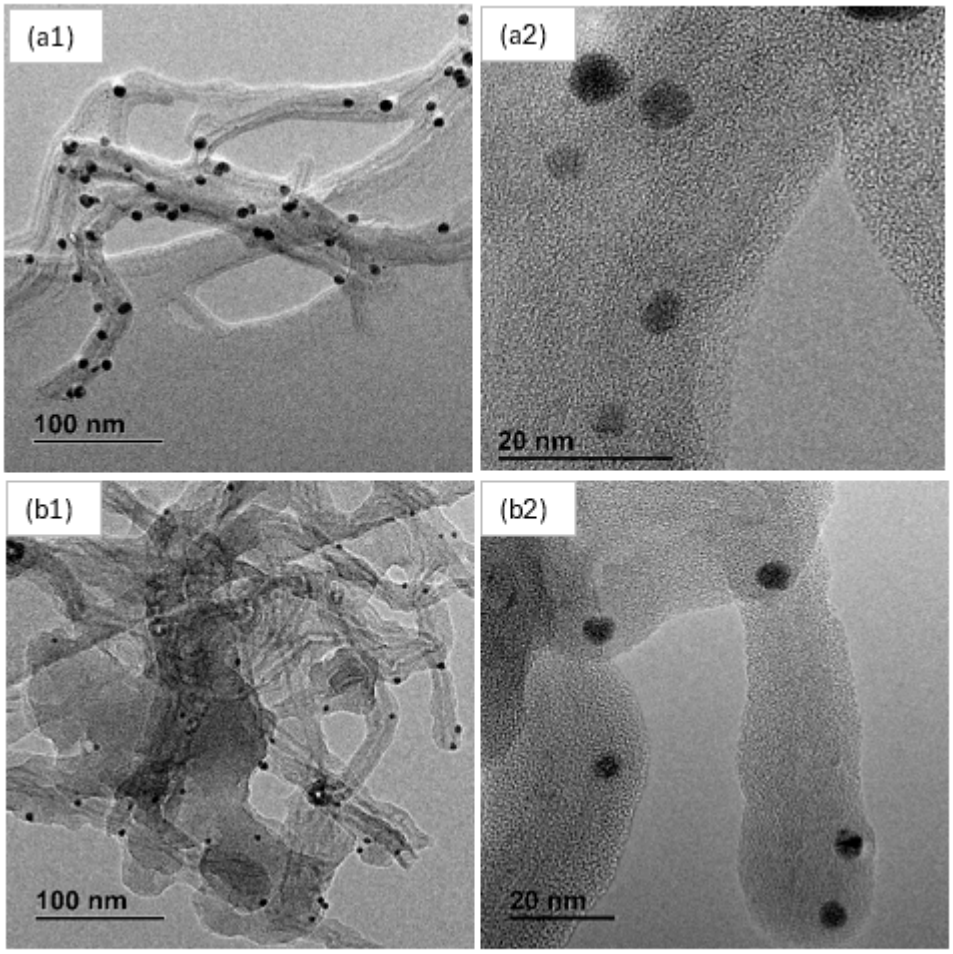

Figure 1. TEM images of (**a1**,**a2**) AgCNT and (**b1**,**b2**) AgP-CNT nanocomposites at lower and higher magnification.

3.1.3. BET Surface Analysis of PVDF-HFP, AgCNT/PVDF-HFP and AgP-CNT/PVDF-HFP Nanocomposite Membranes

The BET specific surface area and pore volume data for the PVDF-HFP, AgCNT/PVDF-HFP and AgP-CNT/PVDF-HFP nanocomposite membranes are presented in Table 1. The PVDF-HFP polymeric membrane had a low surface area of 3.61 m^2g^{-1}; however, after modification with AgCNTs, the surface area increased to 3.71 m^2g^{-1}, which could be associated with the improved hydrophilicity of the entire membrane's structure. The addition of poly(amidoamine) to obtain 1.8 wt.% doping of (AgPCNTs) on PVDF-HFP resulted in a further increase in the BET surface area (3.82 m^2g^{-1}), which could be linked to the improved dispersity of Ag nanoparticles (as demonstrated by TEM data) and the crosslinking of P-MWCNTs with the PVDF-HFP moiety [23]. The nanocomposite membranes showed a type IV(a) isotherm and a sharp capillary condensation step, with pore sizes ranging between 2 and 50 nm (Figure 3 insert). These results indicated that the PVDF-HFP nanocomposite membranes had a mesoporous structure (Figure 3), which was further confirmed by the relative pressure ranging between 0.8 and 0.99 [34].

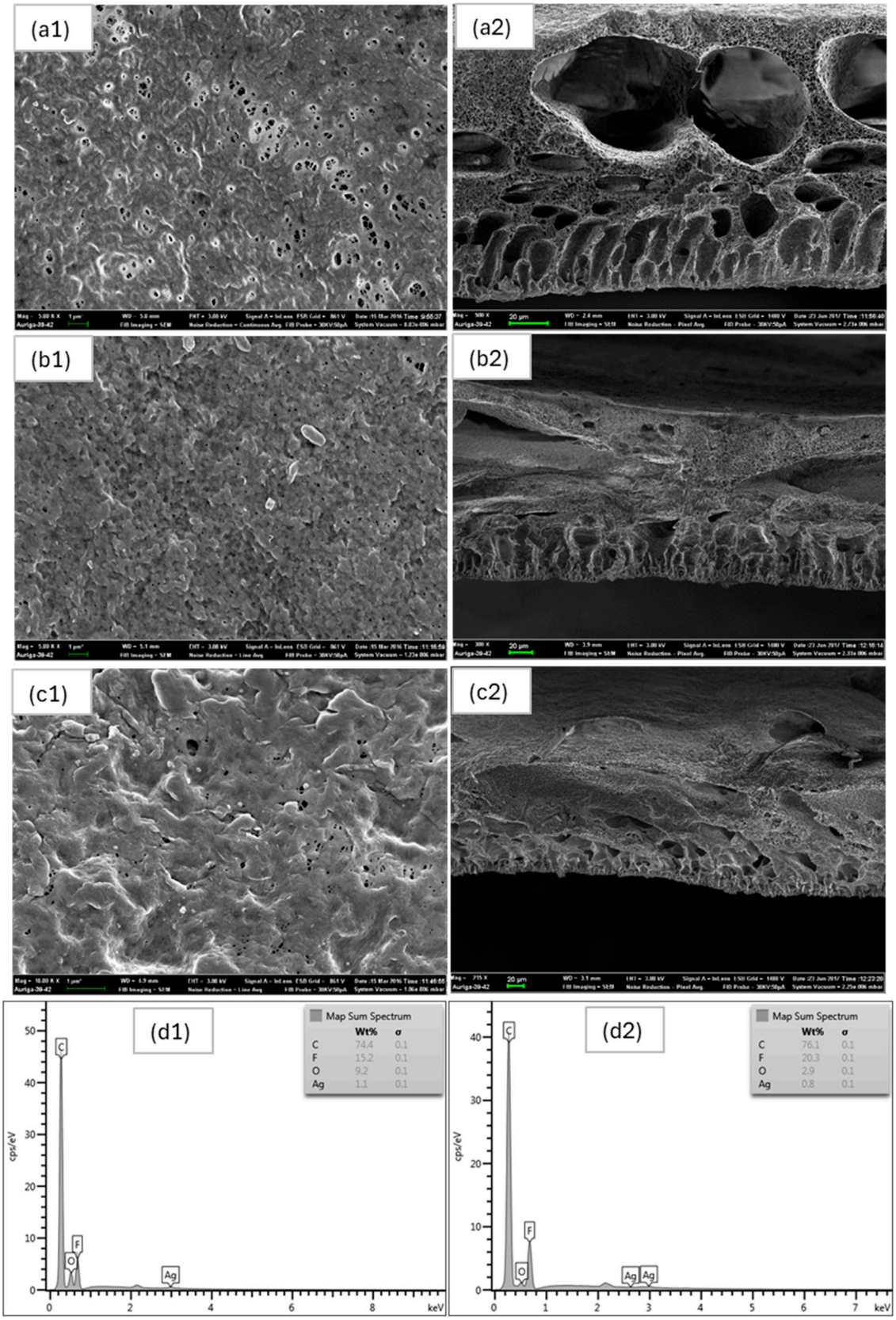

Figure 2. SEM images and cross-sections of (**a1**,**a2**) PVDF-HFP, (**b1**,**b2**) AgCNT/PVDF-HFP and (**c1**,**c2**) AgP-CNT/PVDF-HFP nanocomposite membranes; and EDX of (**d1**) AgCNT/PVDF-HFP and (**d2**) AgP-CNT/PVDF-HFP nanocomposite membranes.

Table 1. Surface characteristics of PVDF-HFP, AgCNT/PVDF-HFP and AgP-CNT/PVDF-HFP nanocomposite membranes.

Sample Name	BET Surface Area (m^2g^{-1})	Total Pore Volume (cm^3g^{-1})
PVDF-HFP	3.61	0.0094
AgCNT/PVDF-HFP	3.71	0.0098
AgPCNT/PVDF-HFP	3.82	0.0148

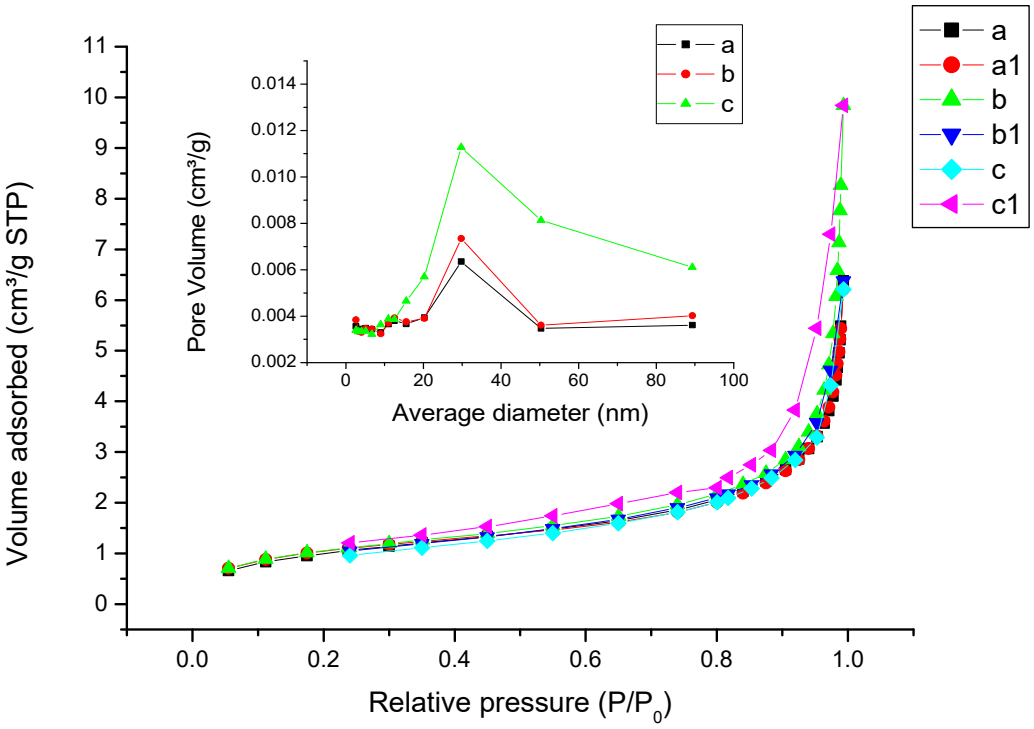

Figure 3. Nitrogen adsorption and desorption isotherms and BJH pore size distribution of (a) PVDF-HFP, (b) AgCNT/PVDF-HFP-MWCNT and (c) AgP-CNT/PVDF-HFP membranes.

3.1.4. TGA Results of PVDF-HFP, AgCNT/PVDF-HFP and AgP-CNT/PVDF-HFP Nanocomposite Membranes

Figure 4 shows the TGA profiles of the AgCNT, AgP-CNT, PVDF-HFP, AgCNT/PVDF-HFP and AgP-CNT/PVDF-HFP nanocomposite membranes. The TGA profile of Ag/MWCNTs shows a weight loss of approximately 34%, with the remainder being the Ag nanoparticles. However, in the presence of poly(amidoamine), the AgP-CNT nanocomposite showed a weight loss of approximately 68% at 700 °C, which suggests a silver loading of about 32%. The decomposition of the poly(amidoamine) moiety and carbon nanotube body were indicated by the weight loss at 330 and 460 °C, respectively, and this was comparable to the work reported in the literature [35]. PVDF-HFP showed weight loss from 200 to 350 °C, followed by the third step at 400 °C. Interestingly, the TGA profile of AgP-CNT/PVDF-HFP showed improved stability as compared to that of AgCNT/PVDF-HFP, due to the presence of the poly(amidoamine) dendrimer. The two nanocomposite membranes exhibited a sudden weight loss at about 450 °C, which was attributed to the structural loss of the PVDF-HFP nanocomposite, as reported in the literature [36].

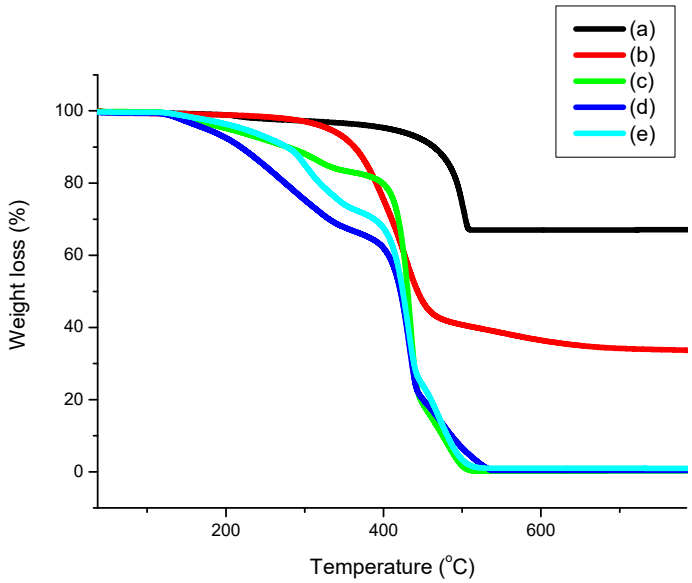

Figure 4. TGA profiles of (a) AgCNT, (b) AgP-CNT, (c) PVDF-HFP, (d) AgCNT/PVDF-HFP and (e) AgP-CNT/PVDF-HFP nanocomposites.

3.1.5. Permeation Tests of PVDF-HFP Nanocomposite Membranes

The permeation studies were undertaken by monitoring the swellability, porosity, water content and contact angle of the PVDF-HFP membranes, as shown in Table 2. AgP-CNT/PVDF-HFP showed an increase in porosity, swellability and water content, when compared to both the PVDF-HFP and AgCNT/PVDF-HFP membranes, which indicates an improvement in hydrophilicity. These results were further supported by a decrease in the contact angle from 78 to 64°, after the addition of AgP-CNTs to PVDF-HFP.

Table 2. Structural features of PVDF-HFP nanocomposite membranes.

Type of Membrane	Porosity (%)	Swellability (%)	Water Content (%)	Contact Angle
PVDF-HFP	70	12	61	78 ± 1.5°
AgCNT/PVDF-HFP	87	17	88	67 ± 2.2°
AgP-CNT/PVDF-HFP	90	18	89	64 ± 1.6°

3.2. Analysis of Surface Water Samples

Table 3 shows the physicochemical properties of the surface water before and after treatment with the PVDF-HFP-based membranes. This was undertaken to evaluate the efficacy of the membranes during water purification. Although the conductivity of the raw surface water was already compliant with the SANS 241 [8] and WHO [6] guidelines, it was reduced by 2.6- and 4-fold after membrane filtration when using AgCNT/PVDF-HFP and AgP-CNT/PVDF-HFP, respectively (Table 3). Furthermore, the nanocomposite membranes' filters significantly improved the colour of the surface water to produce transparent water, which is desirable as colour is an important aesthetic property of drinking water [8]. The turbidity and total suspended solids were higher than the acceptable limits in all raw river water samples [37]. Interestingly, after membrane treatment, the particulate suspended materials and dissolved substances contained in the surface water were significantly reduced. This observation was supported by the large decreases in parameters such as turbidity, TSS and TDS (Table 3), as reported in the literature [14].

Table 3. Physicochemical properties of surface water samples before and after membrane filtration treatment.

Parameter		Raw Water	* Membrane 1 (Fold Decrease)	** Membrane 2 (Fold Decrease)	SANS 241 Guidelines [8]	WHO [6]
Conductivity (mS/m)		63.5	24.1 (2.6)	15.1 (4.2)	≤170	≤250
Colour mg/L Pt-Co	Apparent colour	3.0	0.6 (5)	0.3 (10)	≤15	≤15
	True colour	0.3	0.6 (0.5)	0.2 (1.5)	≤15	≤6
Turbidity (NTU)		21	1 (21)	4 (5.3)	≤5	≤5
TSS (mg/L)		28	8 (3.5)	7 (4)	≤5	≤5
pH		8.15	7.5 (1)	7.26 (1.1)	≥5 to ≤9.7	≥6.5 to ≤8.5
TDS (mg/L)		320	121 (2.6)	7.69 (42)	≤1200	≤1000
Carbonate hardness (mg/L)		10.4	2.3 (4.5)	5.9 (1.8)	≤150	≤100
BOD (mg/L)		27.8	3.8 (7.3)	3.0 (9.3)	-	-

* Membrane 1 is AgCNT/PVDF-HFP and ** Membrane 2 is AgP-CNT/PVDF-HFP.

The pH was within an acceptable range, between 5 and 9.7 (Table 3), indicative of alkaline water. Treatment with the AgP-CNT/PVDF-HFP nanocomposite membranes neutralised the pH of the treated water samples. The TDS is directly proportional to the electrical conductivity and it is influenced by the type and amount of dissolved inorganic salts [38]. The TDS and carbonate hardness were also significantly reduced to acceptable limits [6,8], which indicates the effectiveness of the membranes in improving the purity of surface water.

The BOD measurements of the raw water were greatly reduced after filtration, and this proved the efficacy of the AgP-CNT/PVDF-HFP nanocomposite membranes. Such water with a low BOD can remain safer for a longer time because the low level of organic matter results in low levels of nutrients for microbial growth. A 5-day BOD that falls between 1 and 2 mg/L indicates very clean water, 3 to 5 mg/L indicates moderately clean water and over 8 mg/L indicates severely polluted water [38]. The physicochemical evaluation of the treated water indicated that the water quality was improved by both the AgP-CNT/PVDF-HFP and AgCNT/PVDF-HFP nanocomposite membranes. Interestingly, water samples treated with the AgP-CNT/PVDF-HFP nanocomposite membrane gave even better results compared to the Ag-CNT/PVDF-HFP nanocomposite membrane.

3.3. Microbial Analysis of the Collected Surface Water Samples

3.3.1. Microbial Analysis

The enteric bacteria, *E. coli*, total coliforms and aerobic count were analysed in the surface water samples collected from the Sekhukhune district and are recorded in Table 4. The microbiological quality of the surface water was found to be poor; hence, it was not suitable for home use and had to be treated before consumption by humans. Following treatment with the AgCNT/PVDF-HFP nanocomposite membrane, the levels of enteric bacteria, *E. coli*, total coliforms and aerobic count were reduced to 21, 0, 21 and $>4.9 \times 10^5$, respectively. However, upon treatment with the AgP-CNT/PVDF-HFP nanocomposite membrane, the levels of enteric bacteria, *E. coli*, total coliforms and aerobic count were all reduced to zero. These results indicate that the quality of the water samples was improved to acceptable levels for all classes of microorganisms when filtered with the AgP-CNT/PVDF-HFP nanocomposite membrane, which is attributed to its high BET surface area (Table 1) [16].

Table 4. Levels of bacteria in surface water samples before and after membrane treatment.

Parameter	Raw Water	* Membrane 1	** Membrane 2	SANS 241 Guidelines [8]	WHO [6]
Enterobacteriaceae (CFU/mL)	89	21	0	not specified	not specified
E. coli count (CFU/100 mL)	10	0	0	undetectable	undetectable
Total coliform count (CFU/100 mL)	105	21	0	≤10	≤200
Aerobic count (CFU/mL)	$>4.9 \times 10^5$	$>4.9 \times 10^5$	0	≤1000	≤1000

* Membrane 1 is AgCNT/PVDF-HFP and ** Membrane 2 is AgP-CNT/PVDF-HFP.

3.3.2. Surface Water Heavy Metal Analysis

Table 5 shows the elemental analysis of the water samples measured using atomic adsorption spectroscopy (AAS) before and after membrane filtration. The data in Table 5 show that the levels of chromium, nickel and cadmium were above the acceptable levels of the SANS 241 and WHO [6,8]. The levels of chromium and nickel were relatively similar to those reported in Dzindi [13], the Olifants river [10] and the Durban wastewater treatment plant [9]. The heavy metal analysis indicates that the surface water from the Sekhukhune district is not suitable for consumption if not treated. Fortunately, the concentrations of copper, iron and zinc in the water from Sekhukhune district were within the recommended levels for drinkable water, although zinc was below the detection limit of AAS.

Table 5. Elemental analysis of surface water before and after membrane treatment.

Parameter	Raw Pooled Water (mg/L)	Treated Water (mg/L)				Guidelines (mg/L)	
		* Membrane 1	% Reduction	** Membrane 2	% Reduction	SANS 241 [8]	WHO [6]
Zinc	BDL	-	-	-	-	≤5	≤3
Copper	0.018	0.0011	93%	0.002	89%	≤2	≤2
Iron	0.512	0.003	99%	0.002	99%	≤2	≤0.1
Chromium	0.194	0.0160	92%	0.0138	93%	≤0.05	≤0.05
Cadmium	0.057	0.0028	95%	0.0012	98%	≤0.003	≤0.003
Nickel	0.099	0.027	73%	0.0150	85%	≤0.07	≤0.02

* Membrane 1 is AgCNT/PVDF-HFP, ** Membrane 2 is AgP-CNT/PVDF-HFP and BDL is defined as 'below detection limit'.

Interestingly, upon filtration with the AgCNT/PVDF-HFP nanocomposite membrane, the concentration levels of nickel, cadmium and chromium were reduced by 73, 95 and 92%, respectively. Further reductions in nickel, cadmium and chromium (85, 98 and 93%, respectively) were noted when using the AgP-CNT/PVDF-HFP nanocomposite membrane. This improved removal efficiency is associated with the higher specific surface area of the nanocomposite, due to the presence of the poly(amidoamine) dendrimer, as observed elsewhere [23]. The data thus far evidently support the efficacy of the membranes in improving the quality of water for household use.

Furthermore, a comparison of a variety of nanoparticles and nanocomposite materials is shown in Table 6. The AgP-CNT/PVDF-HFP nanocomposite membrane showed better heavy metal reduction, providing levels that fall within the limits set by the SANS 241 [8] and WHO [6] guidelines [15,16,39]. This nanocomposite membrane also demonstrated good microbial reduction that was comparable with the work reported in the literature [16].

Table 6. Comparison of some nanocomposites in removal of microbial and heavy metals.

Membrane/ Nanoadsorbent	Experimental Conditions	Parameter			Reference
		BOD (mg/L)	Microbial	Heavy Metals (mg/L)	
CuO-NPs	-	87.2%	-	Cr = 91.4% Cd = 64.4%	[39]
Ag nanoparticles	pH = 7.87	181.53 (56%)	-		[14]
Copper–zeolite composite	-		Total coliforms = 100%	Cr = BDL Cd = 0.005	[16]
Kaolin/ZnO	-	94%	-	Cr = 100% Fe = 98%	[15]
(AgP-CNT)/PVDF-HFP	pH = 8.15	3.0 (89%)	*E. coli* = 100% Total coliforms = 100%	Cr = 0.0138 (93%) Fe = 0.002 (99%) Cd = 0.0012 (98%)	Present study
(Ag-CNT)/PVDF-HFP	pH = 8.15	3.8 (86%)	*E. coli* = 100% Total coliforms = 80%	Cr = 0.0160 (92%) Fe = 0.003 (99%) Cd = 0.0028 (95%)	Present study

Following the filtration analysis, the surface of the AgP-CNT/PVDF-HFP nanocomposite membrane was further investigated using the SEM and EDX techniques (Figure 5a,b). The surface of the membrane appeared rougher, mainly due to suspended particles with sizes ranging between 5 and 20 µm (Figure 5a). This is consistent with the removal of the total suspended solids from the surface water, as depicted in Table 3. When the surface of the membrane was studied by EDX, most of the investigated metals were detected; these results correlated with the AAS data reported in Table 5. In our previous studies, it was shown that these types of membranes can be easily regenerated and are not easily fouled [21,40].

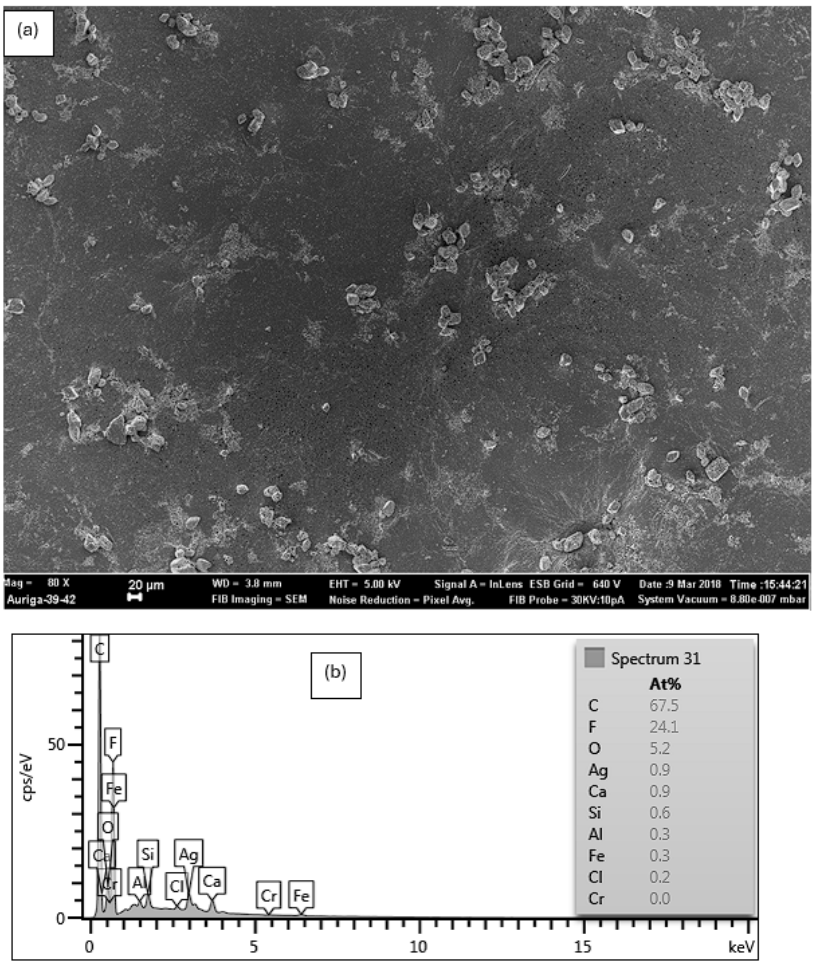

Figure 5. (**a**) SEM and (**b**) EDX of AgP-CNT/PVDF-HFP nanocomposite membranes after filtering surface water samples.

4. Conclusions

The TEM and EDX analysis confirmed the presence of Ag nanoparticles with diameters ranging between 5 and 7 nm on the surfaces of the AgP-CNT/PVDF-HFP nanocomposite membranes. The presence of the poly(amidoamine) dendrimer improved the dispersity of the Ag nanoparticles, as well as the stability of the nanocomposite membrane. This was further confirmed by the TEM and TGA data, as well as the increased BET surface area. SEM images showed the spongy morphology on the surfaces of the nanocomposite membranes, with pores well distributed on the surface. The AgP-CNT/PVDF-HFP nanocomposite membrane demonstrated efficacy in improving the physicochemical and microbiological properties of contaminated river water in the water purification analysis, thus rendering the water potable and suitable for human use. The nanocomposite membranes significantly reduced the physicochemical parameters, such as the conductivity, colour, turbidity, TSS, pH, TDS and carbonate hardness, within the sampled surface waters. Furthermore, it is important to mention the improvements in the microbial load, BOD and heavy metal reduction after the membrane filtration of the surface water samples. In the present study, the AgP-CMTs/PVDF-HFP nanocomposite membranes significantly reduced both the microbial load and heavy metals in the surface water samples.

Author Contributions: Conceptualisation, L.E.M., K.L.M.M. and T.M.; methodology, L.E.M.; investigation, L.E.M.; writing—original draft preparation, L.E.M.; writing—review and editing, L.E.M., K.L.M.M. and T.M.; project administration, T.M. All authors have read and agreed to the published version of the manuscript.

Funding: This research was funded by the National Research Foundation (NRF), grant number SFH13082931704.

Data Availability Statement: All data used during the study appear in the submitted article.

Acknowledgments: We would like to acknowledge the support of this work by the Department of Chemistry and the Department of Biochemistry, Microbiology and Biotechnology, University of Limpopo.

Conflicts of Interest: The authors declare no conflicts of interest.

References

1. Edokpayi, J.N.; Rogawski, E.T.; Kahler, D.M.; Hill, C.L.; Reynolds, C.; Nyathi, E.; Smith, J.A.; Odiyo, J.O.; Samie, A.; Bessong, P.; et al. Challenges to Sustainable Safe Drinking Water: A Case Study Ofwater Quality and Use across Seasons in Rural Communities in Limpopo Province, South Africa. *Water* **2018**, *10*, 159. [CrossRef] [PubMed]
2. Varkey, A.J. Purification of River Water Using Moringa Oleifera Seed and Copper for Point-of-Use Household Application. *Sci. Afr.* **2020**, *8*, e00364. [CrossRef]
3. Genthe, R.; Kfir, R. *Studies on Microbiological Drinking*; WRC Project No. 469/1/95; Water Research Commission: Pretoria, South Africa, 1992.
4. Halkman, H.B.D.; Halkman, A.K. *Indicator Organisms*, 2nd ed.; Elsevier: Amsterdam, The Netherlands, 2014; Volume 2, ISBN 9780123847331.
5. Li, D.; Liu, S. Water Quality Monitoring in Aquaculture. *Water Qual. Monit. Manag.* **2019**, *1*, 303–328. [CrossRef]
6. Herschy, R.W. Water Quality for Drinking: WHO Guidelines. In *Encyclopedia of Lakes and Reservoirs*; Springer: Dordrecht, The Netherlands, 2012; pp. 876–883. [CrossRef]
7. American Public Health Association. APHA Method 9221: Standard Methods for the Examination of Water and Wastewater. *Am. Phys. Educ. Rev.* **1998**, *24*, 481–486.
8. *SANS 241-1*; 2011 South African National Standard,Drinking Water Part 1: Microbiological, Physical, Aesthetic. Alabbott: Pretoria, South Africa, 2011. Available online: https://alabbott.co.za/wp-content/uploads/2020/02/abbott_sans_241_test_requirements.pdf (accessed on 20 February 2019).
9. Bakare, B.F.; Adeyinka, G.C. Evaluating the Potential Health Risks of Selected Heavy Metals across Four Wastewater Treatment Water Works in Durban, South Africa. *Toxics* **2022**, *10*, 340. [CrossRef]
10. Atangana, E.; Oberholster, P.J. Using Heavy Metal Pollution Indices to Assess Water Quality of Surface and Groundwater on Catchment Levels in South Africa. *J. Afr. Earth Sci.* **2021**, *182*, 104254. [CrossRef]
11. Jaishankar, M.; Tseten, T.; Anbalagan, N.; Mathew, B.B.; Beeregowda, K.N. Toxicity, Mechanism and Health Effects of Some Heavy Metals. *Interdiscip. Toxicol.* **2014**, *7*, 60–72. [CrossRef]

12. Addo-Bediako, A. Assessment of Heavy Metal Pollution in the Blyde and Steelpoort Rivers of the Olifants River System, South Africa. *Polish J. Environ. Stud.* **2020**, *29*, 3023–3029. [CrossRef]
13. Edokpayi, J.N.; Odiyo, J.O.; Olasoji, S.O. Assessment of Heavy Metal Contamination of Dzindi River, in Limpopo Province, South Africa. *Int. J. Nat. Sci. Res.* **2014**, *2*, 185–194.
14. Eid, A.M.; Fouda, A.; Hassan, S.E.D.; Hamza, M.F.; Alharbi, N.K.; Elkelish, A.; Alharthi, A.; Salem, W.M. Plant-Based Copper Oxide Nanoparticles; Biosynthesis, Characterization, Antibacterial Activity, Tanning Wastewater Treatment, and Heavy Metals Sorption. *Catalysts* **2023**, *13*, 348. [CrossRef]
15. Mustapha, S.; Tijani, J.O.; Ndamitso, M.M.; Abdulkareem, S.A.; Shuaib, D.T.; Mohammed, A.K.; Sumaila, A. The Role of Kaolin and Kaolin/ZnO Nanoadsorbents in Adsorption Studies for Tannery Wastewater Treatment. *Sci. Rep.* **2020**, *10*, 13068. [CrossRef] [PubMed]
16. Fanta, F.T.; Dubale, A.A.; Bebizuh, D.F.; Atlabachew, M. Copper Doped Zeolite Composite for Antimicrobial Activity and Heavy Metal Removal from Waste Water. *BMC Chem.* **2019**, *13*, 44. [CrossRef] [PubMed]
17. Shannon, M.A.; Bohn, P.W.; Elimelech, M.; Georgiadis, J.G.; Mariñas, B.J.; Mayes, A.M. Science and Technology for Water Purification in the Coming Decades. *Nature* **2008**, *452*, 301–310. [CrossRef] [PubMed]
18. Zhang, C.; Wei, K.; Zhang, W.; Bai, Y.; Sun, Y.; Gu, J. Graphene Oxide Quantum Dots Incorporated into a Thin Film Nanocomposite Membrane with High Flux and Antifouling Properties for Low-Pressure Nanofiltration. *ACS Appl. Mater. Interfaces* **2017**, *9*, 11082–11094. [CrossRef]
19. Wei, X.; Shi, Y.; Fei, Y.; Chen, J.; Lv, B.; Chen, Y.; Zheng, H.; Shen, J.; Zhu, L. Removal of Trace Phthalate Esters from Water by Thin-Film Composite Nanofiltration Hollow Fiber Membranes. *Chem. Eng. J.* **2016**, *292*, 382–388. [CrossRef]
20. Somma, S.; Reverchon, E.; Baldino, L. Water Purification of Classical and Emerging Organic Pollutants: An Extensive Review. *ChemEngineering* **2021**, *5*, 47. [CrossRef]
21. Macevele, L.E.; Moganedi, K.L.M.; Magadzu, T. Investigation of Antibacterial and Fouling Resistance of Silver and Multi-Walled Carbon Nanotubes Doped Poly(Vinylidene Fluoride-Co-Hexafluoropropylene) Composite Membrane. *Membranes* **2017**, *7*, 35. [CrossRef]
22. Santos, A.; Veiga, F.; Figueiras, A. Dendrimers as Pharmaceutical Excipients: Synthesis, Properties, Toxicity and Biomedical Applications. *Materials* **2020**, *13*, 65. [CrossRef]
23. Kahu, S.S.; Shekhawat, A.; Saravanan, D.; Jugade, R.M. Two Fold Modified Chitosan for Enhanced Adsorption of Hexavalent Chromium from Simulated Wastewater and Industrial Effluents. *Carbohydr. Polym.* **2016**, *146*, 264–273. [CrossRef]
24. Li, G.; Shen, L.; Luo, Y.; Zhang, S. The Effect of Silver-PAMAM Dendrimer Nanocomposites on the Performance of PVDF Membranes. *Desalination* **2014**, *338*, 115–120. [CrossRef]
25. Yuan, W.; Jiang, G.; Che, J.; Qi, X.; Xu, R.; Chang, M.W.; Chen, Y.; Lim, S.Y.; Dai, J.; Chan-Park, M.B. Deposition of Silver Nanoparticles on Multiwalled Carbon Nanotubes Grafted with Hyperbranched Poly(Amidoamine) and Their Antimicrobial Effects. *J. Phys. Chem. C* **2008**, *112*, 18754–18759. [CrossRef]
26. Rajesh, R.; Venkatesan, R. Encapsulation of Silver Nanoparticles into Graphite Grafted with Hyperbranched Poly(Amidoamine) Dendrimer and Their Catalytic Activity towards Reduction of Nitro Aromatics. *J. Mol. Catal. A Chem.* **2012**, *359*, 88–96. [CrossRef]
27. Mpala, T.J.; Richards, H.; Etale, A.; Mahlangu, O.T.; Nthunya, L.N. Carbon Nanotubes and Silver Nanoparticles Modification of PVDF Membranes for Improved Seawater Desalination in Direct Contact Membrane Distillation. *Front. Membr. Sci. Technol.* **2023**, *2*, 1–11. [CrossRef]
28. Makhuvele, R.; Moganedi, K.L.M. Efficiency and Applicability of Low Cost Home-Based Water Treatment Strategies in a Rural Context. *J. Biol. Sci.* **2019**, *19*, 339–346. [CrossRef]
29. Zhao, W.; Wang, H.; Qin, X.; Wang, X.; Zhao, Z.; Miao, Z.; Chen, L.; Shan, M.; Fang, Y.; Chen, Q. A Novel Nonenzymatic Hydrogen Peroxide Sensor Based on Multi-Wall Carbon Nanotube/Silver Nanoparticle Nanohybrids Modified Gold Electrode. *Talanta* **2009**, *80*, 1029–1033. [CrossRef]
30. Larrude, D.G.; Maia Da Costa, M.E.H.; Freire, F.L. Synthesis and Characterization of Silver Nanoparticle-Multiwalled Carbon Nanotube Composites. *J. Nanomater.* **2014**, *2014*, 654068. [CrossRef]
31. Wang, X.; Xiao, C.; Liu, H.; Huang, Q.; Hao, J.; Fu, H. Poly(Vinylidene Fluoride-Hexafluoropropylene) Porous Membrane with Controllable Structure and Applications in Efficient Oil/Water Separation. *Materials* **2018**, *11*, 443. [CrossRef] [PubMed]
32. Shi, L.; Wang, R.; Cao, Y.; Feng, C.; Liang, D.T.; Tay, J.H. Fabrication of Poly(Vinylidene Fluoride-Co-Hexafluropropylene) (PVDF-HFP) Asymmetric Microporous Hollow Fiber Membranes. *J. Memb. Sci.* **2007**, *305*, 215–225. [CrossRef]
33. Rajesh, S.; Maheswari, P.; Senthilkumar, S.; Jayalakshmi, A.; Mohan, D. Preparation and Characterisation of Poly (Amide-Imide) Incorporated Cellulose Acetate Membranes for Polymer Enhanced Ultrafiltration of Metal Ions. *Chem. Eng. J.* **2011**, *171*, 33–44. [CrossRef]
34. Mkhondo, N.B.; Magadzu, T. Effects of Different Acid-Treatment on the Nanostructure and Performance of Carbon Nanotubes in Electrochemical Hydrogen Storage. *Dig. J. Nanomater. Biostruct.* **2014**, *9*, 1331–1338.
35. Salam, M.A.; Burk, R. Synthesis and Characterization of Multi-Walled Carbon Nanotubes Modified with Octadecylamine and Polyethylene Glycol. *Arab. J. Chem.* **2017**, *10*, S921–S927. [CrossRef]
36. Gsaiz, P.; Lopes, A.C.; Eizagirre, S.; De Luis, R.F.; Isabel, M. Ionic Liquids for the Control of the Morphology in Poly (Vinylidene Fluoride-Co-Hexafluoropropylene) Membranes. *Mater. Des.* **2018**, *155*, 325–333. [CrossRef]

37. Macevele, L.E.; Lydia, K.; Moganedi, M.; Magadzu, T. Adsorption of Cadmium (II) Ions from Aqueous Solutions Using Poly (Amidoamine)/Multi-Walled Carbon Nanotubes Doped Poly (Vinylidene Fluoride-Co-Hexafluoropropene) Composite Membrane. *J. Membr. Sci. Res.* **2021**, *7*, 152–165. [CrossRef]
38. Ahmed, T.; Noman, M.; Shahid, M.; Niazi, M.B.K.; Hussain, S.; Manzoor, N.; Wang, X.; Li, B. Green Synthesis of Silver Nanoparticles Transformed Synthetic Textile Dye into Less Toxic Intermediate Molecules through LC-MS Analysis and Treated the Actual Wastewater. *Environ. Res.* **2020**, *191*, 110142. [CrossRef]
39. Sharma, S.; Bhattacharya, A. Drinking Water Contamination and Treatment Techniques. *Appl. Water Sci.* **2017**, *7*, 1043–1067. [CrossRef]
40. Rice, E.W.; Bridgewater, L.; American Public Health Association (Eds.) *Standard Methods for the Examination of Water and Wastewater*; American Public Health Association: Washington, DC, USA, 2012; p. 1496.